MOLECULAR AND CELLULAR BIOLOGY, July 1986, p. 2582–2592
0270-7306/86/072582-11$02.00/0

Vol. 6, No. 7

Ribonucleoprotein Complex Formation during Pre-mRNA Splicing In Vitro

ALBRECHT BINDEREIF AND MICHAEL R. GREEN

Department of Biochemistry and Molecular Biology, Harvard University, Cambridge, Massachusetts 02138

Received 6 February 1986/Accepted 3 April 1986

The ribonucleoprotein (RNP) structures of the pre-mRNA and RNA processing products generated during in vitro splicing of an SP6/β-globin pre-mRNA were characterized by sucrose gradient sedimentation analysis. Early, during the initial lag phase of the splicing reaction, the pre-mRNA sedimented heterogeneously but was detected in both 40S and 60S RNP complexes. An RNA substrate lacking a 3′ splice site consensus sequence was not assembled into the 60S RNP complex. The two splicing intermediates, the first exon RNA species and an RNA species containing the intron and the second exon in a lariat configuration (IVS1-exon 2 RNA species), were found exclusively in a 60S RNP complex. These two splicing intermediates cosedimented under a variety of conditions, indicating that they are contained in the same RNP complex. The products of the splicing reaction, accurately spliced RNA and the excised IVS1 lariat RNA species, are released from the 60S RNP complex and detected in smaller RNP complexes. Sequence-specific RNA-factor interactions within these RNP complexes were evidenced by the preferential protection of the pre-mRNA branch point from RNase A digestion and protection of the 2′-5′ phosphodiester bond of the lariat RNA species from enzymatic debranching. The various RNP complexes were further characterized and could be distinguished by immunoprecipitation with anti-Sm and anti-(U1)RNP antibodies.

Most structural genes in higher eucaryotes contain intervening sequences that are removed from the primary transcripts (pre-mRNAs) by splicing. The development of in vitro splicing systems (11, 12, 16, 24) has led to rapid progress in understanding the biochemistry and mechanism of the splicing reaction. Based on the kinetics of splicing in vitro (9, 16) and the structural characterization of in vitro-generated RNA processing products (25, 32), a two-stage splicing pathway has been formulated. In the first stage, the pre-mRNA is cleaved at the 5′ splice site to generate two splicing intermediates: the first-exon RNA species and an RNA species composed of the intron and the second exon (IVS1-exon 2 RNA species). In the second stage, cleavage at the 3′ splice site and ligation of the exons occurs, producing accurately spliced RNA and the excised IVS1. The excised IVS1 and IVS1-exon 2 RNA species are in the form of a lariat in which the 5′ end of IVS1 is joined to an adenosine residue near the 3′ end of IVS1 by a 2′-5′ phosphodiester bond (13, 25, 32). Analysis of RNA processing products in mammalian (37) and yeast (6, 28) cells strongly suggests that pre-mRNA splicing also proceeds by this pathway in vivo.

Although significant progress has been made in understanding the biochemistry and mechanism of the splicing reaction, still relatively little is known about how accurate splice site selection is achieved. The consensus sequences at the 5′ and 3′ splice junctions (2, 7, 18, 22, 33), although important for splicing (for a review, see reference 34) are insufficient to account for the accuracy of splice site selection; sequences that conform to the splice junction consensus sequences are found in other pre-mRNA regions but are not selected (for an example, see reference 22). Thus, it is possible that other sequence elements or a higher-order structure of the pre-mRNA is critical for accurate splicing.

One level of higher-order structural organization that may be important is the assembly of pre-mRNA into a ribonucleoprotein (RNP) particle. A variety of electron microscopic and biochemical studies indicate that in vivo heterogeneous nuclear RNA, including nascent RNA, is not naked but is instead complexed to proteins to form RNP complexes referred to as hnRNPs (for a review, see reference 20). These hnRNPs contain six major polypeptides that have been characterized in some detail (20 and references therein). Although the biochemical function of these hnRNP proteins is completely unknown, they may be related to and essential for RNA processing.

Several features of in vitro splicing suggest that pre-mRNA is assembled into an RNP complex early during the splicing reaction. First, in vitro splicing proceeds with a 20- to 45-min lag during which ATP-dependent events occur that are required for subsequent processing (11, 12, 16). This may reflect the time required to assemble the pre-mRNA into an RNP complex, which is the actual splicing substrate. Second, a mechanism is required to ensure that the two splicing intermediates, the first exon and IVS1-exon 2 RNA species, can efficiently give rise to the splicing products. As has been previously postulated, a likely mechanism is that these two RNA species are held together in a complex (25, 32).

As a first step to investigate the role of RNP structures in the in vitro splicing reaction, we attempted to identify and characterize the RNP complexes containing the pre-mRNA and RNA processing products. We found that all of the RNA species were in the form of RNP complexes, which can be partially fractionated by sucrose gradient sedimentation. These partially purified RNP complexes bear important structural similarities to the RNP complexes present in the crude in vitro extract. By a similar approach, it has recently been shown in yeast (3) and mammalian cell extracts with an adenovirus major late substrate (8, 10) that the pre-mRNA, splicing intermediates, and products are in the form of rapidly sedimentable RNP complexes. Our results are discussed with regard to these studies and the pre-mRNA splicing mechanism.

* Corresponding author.

MATERIALS AND METHODS

Materials. SP6 RNA polymerase, RNasin, DNase I, and restriction enzymes were from Promega Biotec or New England BioLabs, Inc., RNase T1 was from Calbiochem-Behring, RNase A was from Boehringer Mannheim Biochemicals, and GpppG was from P-L Biochemicals, Inc. [α-^{32}P]UTP (410 Ci/mmol) was purchased from Amersham Corp.

SP6 transcription and in vitro splicing reactions. The following DNA templates were used for transcription: SP64/H$\beta\Delta$6 (16) cut with *Bam*HI, SP6/H$\beta^{\Delta PyAG}$ (31) cut with *Bam*HI, and SP64 (21) cut with *Hga*I. High-specific-activity, ^{32}P-labeled RNAs were synthesized in 27-μl reaction mixtures containing 4 μg of DNA template, 40 mM Tris hydrochloride (pH 7.5), 6 mM $MgCl_2$, 2 mM spermidine, 15 mM dithiothreitol, 0.4 μl of RNasin, and 8 U of SP6 RNA polymerase. [α-^{32}P]UTP (100 μCi) and 160 μM each of the unlabeled nucleoside triphosphates were added. Capping was achieved by reducing the GTP concentration to 37 μM and including 75 μM GpppG in the transcription reaction mixture (5, 13).

In vitro splicing reactions were carried out as previously described (6, 32), in total volumes of 125 (5×) or 250 (10×) μl with 10 ng of high-specific activity RNA per 1× reaction mixture (greater than 10^7 cpm/μg). As indicated, in some experiments polyvinyl alcohol (PVA) was omitted from the splicing reaction. Before analysis by sucrose gradient sedimentation, the reaction mixture was spun at 12,000 × *g* for 3 min, and the supernatant was removed.

Sedimentation analysis. Equal volumes of SB buffer (10 mM HEPES [*N*-2-hydroxyethylpiperazine-*N'*-2-ethanesulfonic acid], pH 8.0, 3 mM $MgCl_2$, 1 mM dithiothreitol, and KCl to adjust to the KCl concentration of the sucrose gradient) were added to 5× or 10× splicing reaction mixtures before they were loaded onto 10-ml 15 to 30% sucrose gradients containing 0.06, 0.2, 0.5, or 0.9 M KCl in SB buffer. Gradients were centrifuged in an SB283 rotor at 40,000 rpm at 4°C for 5 h and collected from the bottom of the centrifuge tube in 19 to 20 fractions of approximately 0.5 ml each. The gradient fractions were frozen and stored at −20°C. RNA was purified from individual fractions and analyzed by denaturing gel electrophoresis (5.6% acrylamide–8.3 M urea). Quantitation was either by Cerenkov counting of the excised band or by densitometric scanning of an autoradiogram. *Escherichia coli* ribosomes (70S), ribosomal subunits (30S and 50S), and ribosomal RNA (16S) served as sedimentation markers. Using different preparations of nuclear extract, we observed in many experiments a slight variability in the sedimentation of the 60S pre-mRNA RNP complex (55S to 70S; see, for example, Fig. 2C and E). For convenience, we will refer to this pre-mRNA RNP complex as the 60S RNP complex.

RNase A and debranching protection assays. A 10× in vitro splicing reaction mixture (20-min time point) was fractionated by centrifugation through a 15 to 30% sucrose gradient in 0.06 M KCl–SB buffer. Pre-mRNA RNP complexes of approximately 60S were isolated and subjected to a partial RNase A digest (10 to 100 ng of RNase A/150-μl gradient fraction for 30 min at 30°C). RNase A-resistant fragments were gel purified, digested with RNase T1, and fractionated by denaturing gel electrophoresis. The RNase T1 fragments were purified and digested with RNase A. The RNase A digestion products were fractionated by two-dimensional thin-layer chromatography on polyethyleneimine plates (32, 35).

For the debranching protection assay, gradient fractions (30 to 50 μl) were adjusted to 0.1 M KCl and 10 mM EDTA and subjected to the enzymatic debranching reaction (30) by adding 10 μl of HeLa cell cytoplasmic S100 fraction. After 30 min at 30°C, the RNA was purified and analyzed by denaturing gel electrophoresis.

Immunoprecipitation. Anti-Sm and anti-(U1)RNP sera were obtained from the Centers for Disease Control (Atlanta, Ga.) and diluted 1:10 in phosphate-buffered saline (100 mM NaCl, 20 mM potassium phosphate, pH 7.0) before use. Sera were also kindly provided by V. Agnello (Lahey Clinic Medical Center, Burlington, Mass.). These sera were tested for their ability to immunoprecipitate specific ^{32}P-labeled snRNPs prepared from HeLa cells as previously described (19). All sera used in these studies immunoprecipitated the snRNPs expected from their specificity (19). Immunoprecipitations were performed in antibody excess by using aliquots of the gradient fractions essentially as described by Black et al. (1). Portions (100 μl) of the gradient fractions were added to 1 μl of RNasin (Promega Biotech) and 2 μl of a 1:10 dilution of the antiserum and incubated for 30 min on ice, and then 50 μl of a 1:1 suspension of protein A–Sepharose CL-4B (7.5 mg; Pharmacia) in NET-2 buffer (50 mM Tris hydrochloride [pH 7.9], 150 mM NaCl, 0.05% Nonidet P-40 [vol/vol], 0.5 mM dithiothreitol) was added, and the mixture was incubated for 15 min on ice. The pellet was washed three times by spinning for 10 s in a Microfuge (Beckman Instruments, Inc.) suspension in 500 μl of NET-2 buffer. RNA was purified from the immunoprecipitate by proteinase K treatment, phenol extraction, and ethanol precipitation. Under these conditions the immunoprecipitation efficiency of ^{32}P-labeled snRNPs was approximately 20%.

RESULTS

The pre-mRNA and RNA processing products are in the form of rapidly sedimentable RNP complexes. To determine whether the pre-mRNA, splicing intermediates and products were in the form of RNP complexes, the 497-nucleotide (nt) ^{32}P-labeled SP6/β-globin pre-mRNA was processed in vitro (16, 32), and the reaction mixture was fractionated by sucrose gradient centrifugation. The [^{32}P]RNA purified from each gradient fraction was analyzed by denaturing polyacrylamide gel electrophoresis. In preliminary experiments we found that the majority of the [^{32}P]RNA in the splicing reaction mixture precipitated out of solution and therefore pelleted in the sucrose gradient (data not shown). The addition of PVA, which is included in the standard splicing reaction mixture to increase splicing efficiency (16), greatly enhanced precipitation (data not shown; see below). Therefore, when PVA was included, the splicing reaction mixture was divided into soluble and insoluble fractions, and only the soluble fraction was analyzed by sucrose gradient sedimentation.

Interestingly, the RNA processing products were differentially distributed in the soluble and insoluble fractions, making it difficult to detect some of the RNP complexes in the presence of PVA (Fig. 1A; see below). Under standard in vitro splicing conditions (60 mM KCl), the two splicing intermediates (155 and 380 RNAs) were enriched in the pellet. In contrast, the excised IVS1 (143 RNA) was preferentially distributed in the supernatant (Fig. 1A). Addition of 200 mM KCl to the splicing reaction mixture solubilized most of the [^{32}P]RNA (data not shown). Furthermore, at this higher ionic strength the [^{32}P]RNA species were distributed equally in the supernatant and pellet (Fig. 1B).

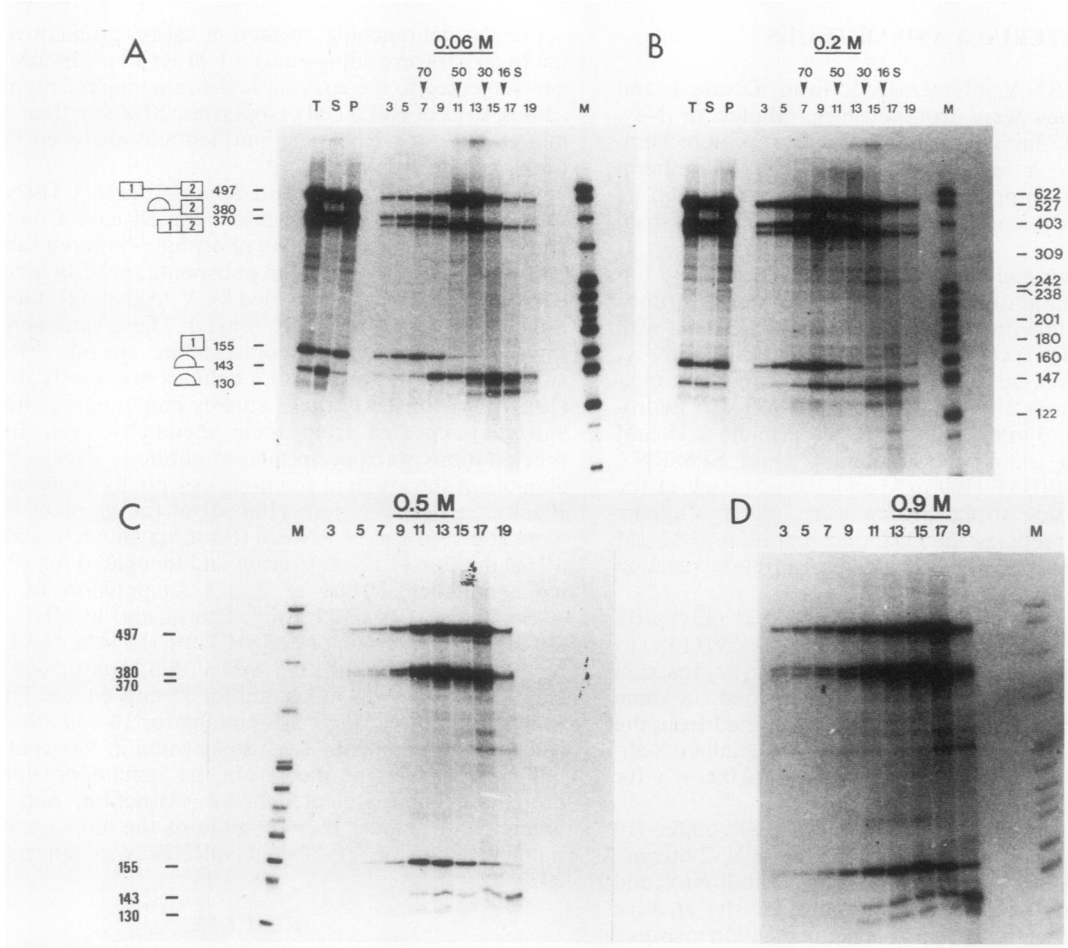

FIG. 1. Sucrose gradient sedimentation analyses of pre-mRNA, splicing intermediates, and product RNPs. ^{32}P-labeled SP64-HβΔ6 RNA (497 nts) was synthesized and spliced in vitro for 90 min, and the reaction mixture was adjusted to the KCl concentrations indicated in the panels (0.06, 0.2, 0.5, and 0.9 M in A, B, C, and D, respectively) and analyzed by sucrose gradient centrifugation. [^{32}P]RNA prepared from the gradient fractions (numbered 1 to 20 from the bottom to the top of the gradient) was resolved by denaturing gel electrophoresis using ^{32}P-labeled *Msp*I-digested pBR322 DNA as markers (M) and detected by autoradiography. The numbers of the gradient fractions and the positions of the sedimentation markers are indicated above the autoradiograms. The RNA species present in the total splicing reaction (T), supernatant (S), and pellet (P) of the 12,000 × *g* centrifugation step was determined by analyzing equal amounts of [^{32}P]RNA from each sample on a denaturing polyacrylamide gel (A and B). A schematic representation (boxes 1 and 2, exons 1 and 2, respectively; line, intron) of pre-mRNA, splicing intermediates, and products, as well as the size of each RNA species, relative to the DNA markers is shown on the left.

A typical sedimentation profile of a 90-min splicing reaction (plus PVA) is shown in Fig. 1A. The 497-nt pre-mRNA sedimented with a peak at 40S but was also distributed throughout the gradient. Significantly, the two splicing intermediates, the 380 and 155 RNAs, were distributed more homogeneously and cosedimented with a peak at 60S. Accurately spliced RNA (370 RNA) was heterogeneously distributed with a broad peak at 25S to 40S. The majority of the excised IVS1 RNA species (143 RNA) was found between 15S and 50S. The 130 RNA species, which is the 143 RNA lacking approximately 10 nts at the linear 3′ end of IVS1 (30), was found in 15S-to-25S RNP complexes.

Under these standard sedimentation conditions, all of the deproteinized [^{32}P]RNA species migrated within the top three fractions (<10S; data not shown). After addition of proteinase K to the in vitro splicing reaction mixture, the RNA species were found within the top three fractions of the gradient (data not shown), indicating that all of the RNA processing products were in fact in RNP complexes.

The sedimentation properties of the various RNP complexes were differentially affected by increasing the ionic strength of the sucrose gradient (Fig. 1B to D). The RNP complex containing the splicing intermediates (380 to 155 RNAs) was most resistant to increased ionic strength; the sedimentation coefficient decreased from 60S (60 mM KCl) to approximately 50S, 40S, and 30S when the KCl concentration was raised to 0.2, 0.5, and 0.9 M, respectively. Significantly, the two splicing intermediates cosedimented at all ionic strengths up to 0.9 M KCl, strongly suggesting that they are contained in the same RNP complex. The RNP complex containing the pre-mRNA sedimented predominantly at 15S to 50S in 0.2 M KCl, at 15S to 40S in 0.5 M KCl, and at 15S in 0.9 M KCl. The RNP complex containing the 370 RNA sedimented at approximately 25S to 35S in 0.2 M salt and at 15S in 0.5 and 0.9 M KCl. The RNP complex containing the 143 RNA was most sensitive to increased ionic strength. This RNP complex migrated at 15S in 0.2 M KCl, and above ionic strengths of 0.5 M KCl it sedimented as naked RNA.

The addition of 10 mM EDTA to the splicing reaction mixture and the sucrose gradients resulted in a shift of the RNP complexes of both the pre-mRNA and splicing inter-

mediates from 60S to 40S–50S (data not shown). Notably, the two splicing intermediates still cosedimented under these conditions.

RNP complex formation at early times during in vitro splicing. To study the involvement of RNP structures in the pre-mRNA splicing mechanism further, we examined the sedimentation of the pre-mRNA RNP complex at an earlier time during in vitro splicing. At 45 min the vast majority of the total [^{32}P]RNA was in the form of pre-RNA; a small amount of the RNA was in the form of splicing intermediates, and no spliced products were detectable. When sucrose gradient centrifugation analysis was performed at this time point (plus PVA), the pre-mRNA RNP complex sedimented at 40S in 60 mM KCl (Fig. 2A), which is indistinguishable from the results obtained at 90 min (Fig. 1). In 200 mM KCl, the pre-mRNA RNP complex sedimented more heterogeneously; two peaks were observed at 20S and 45S (Fig. 2A).

As discussed above, during the course of these studies we noted that inclusion of PVA in the splicing reaction mixture significantly affected detection of the various RNP complexes. For example, if the splicing reaction was performed in the absence of PVA a portion of the pre-mRNA sedimented at 60S (60 mM KCl; Fig. 2C). In contrast, as discussed above, in the presence of PVA a 60S peak could not be detected (Fig. 2A). These results suggest that the large 60S pre-mRNA RNP complex was preferentially precipitated in the presence of PVA. It is likely that the 45S peak observed in 200 mM salt (Fig. 2A) was due to solubilization of the precipitated 60S pre-mRNA RNP complex. Presumably the 40S RNP complex observed in 60 mM KCl was shifted to 20S in 200 mM salt.

To determine whether RNP complex formation is dependent on sequences within eucaryotic pre-mRNAs, we analyzed the sedimentation of a similarly sized RNA (519 nts) derived from *Hga*I-cut plasmid pSP64 (21) after incubation in the crude nuclear extract (minus PVA). This RNA substrate forms RNP complexes of 40S and 20S in 60 and 200 mM KCl sucrose gradients, respectively (Fig. 2D). Significantly, the 60S RNP complex observed with the SP6/β-globin pre-mRNA (Fig. 2C) was not detectable with the pSP64 RNA substrate (Fig. 2D).

ATP is necessary for the production of accurately spliced RNA in vitro (9, 11, 12, 16) and is even required for the first step of splicing, 5′ splice site cleavage and lariat formation (9, 16, 32). To determine whether RNP complex formation is ATP dependent, we compared the sedimentation of the pre-mRNA RNP complex in the presence and absence of ATP (Fig. 2E). Significantly, in the absence of ATP a 60S pre-mRNA RNP complex was not detected, but a 40S RNP complex was still observed. Thus, ATP is required for one or more steps in the assembly of a 60S pre-mRNA RNP complex.

Role of the 3′ splice site in RNP complex formation. Previous studies have demonstrated that the 3′ splice site consensus sequence is required for the first step in mammalian pre-mRNA splicing, 5′ splice site cleavage and lariat formation (8, 27, 31). More recently it has been shown that the 3′ splice site consensus sequence is required for the association of a factor(s) with the RNA branch point (29). These results suggest that the 3′ splice site consensus sequence is required for the formation of a rapidly sedimentable RNP complex. To test this possibility, we analyzed a mutant pre-mRNA (SP6/Hβ$^{\Delta PyAG}$) in which the 3′ splice junction and most of the polypyrimidine tract is deleted but the branch point region is intact (31). In the presence of PVA, the mutant pre-mRNA was present in 40S (60 mM KCl) and 20S (200 mM KCl) RNP complexes (Fig. 2B). This sedimentation behavior is very similar to that observed with the normal pre-mRNA (Fig. 2A). In the absence of PVA, however, no material sedimenting more rapidly than 40S was detected with the mutant pre-mRNA; in contrast, the normal pre-mRNA was present in a 60S RNP complex (Fig. 2C). Thus, the 3′ splice site consensus sequence is an essential *cis*-acting element for the assembly of the 60S RNP complex.

Characterization of the 60S pre-mRNA RNP complexes by protection from RNase A digestion. The results described above indicate that factors are associated with the pre-mRNA and RNA processing products to form rapidly sedimentable RNP complexes. However, these results do not address whether these factors are bound to specific regions of the RNA species. To determine whether the 60S pre-mRNA RNP complexes contain specific RNA-factor interactions, we used protection from RNase A digestion as an assay (29). 60S pre-mRNA RNP complexes formed after 20 min of in vitro splicing were isolated by sucrose gradient sedimentation and subjected to partial RNase A digestion (Fig. 3A, lanes 2 to 4). As a control, deproteinized RNA from the same 60S gradient fraction was partially digested with RNase A under identical conditions. The [^{32}P]RNA in the 60S RNP complex was significantly more resistant to RNase A digestion than was deproteinized pre-mRNA (compare lanes 2 to 4 with lanes 5 to 7). The 60S RNP complex gave rise to multiple RNase A-resistant fragments, the most abundant of which were between 40 and 80 nts (Fig. 3, lanes 3 and 4, RNAs A to D). In contrast, under the same conditions, the purified RNA did not give rise to RNase A-resistant fragments larger than 40 nts (Fig. 3, lanes 6 and 7). Several of the most abundant RNase A-resistant fragments (indicated by arrows) derived from the two RNA substrates were purified and characterized by RNase T1 digestion analysis (Fig. 3B). Significantly, all of the RNase A-resistant fragments derived from the 60S RNP complex (A to D) contained a 10-nt RNase T1 fragment. RNase A secondary digestion analysis (Fig. 3C, 10-mer) unambiguously identified this RNase T1 fragment as ACUCU CUCUG, which is located 26 to 37 nts upstream from the 3′ end of IVS1 and contains the adenosine residue at which the RNA branch forms (32). In contrast, none of the RNase A-resistant fragments derived from the purified RNAs (E to G) contained a 10-nt RNase T1 fragment (Fig. 3B). Analysis of the other RNase T1 fragments derived from the RNase A-resistant fragments A to D allowed construction of a map of the pre-mRNA sequences in the 60S RNP complex protected from RNase A digestion (Fig. 4). Based on these experiments we conclude that the branch point region of the pre-mRNA is preferentially protected from RNase A digestion and that this protection is dependent on protein components of the isolated RNP complex. Preferential protection of sequences at the 3′ end of the intron from nuclease digestion has been previously observed in the crude nuclear extract (1, 4, 29), and the agreement between the two approaches suggests that structurally intact RNP complexes can be isolated by sucrose gradient sedimentation.

Protection of lariat RNA species in RNP complexes from enzymatic debranching. During the in vitro splicing reaction, the 2′-5′ phosphodiester bond of the lariat RNA species is protected from cleavage by endogenous lariat debranching activity (32, 30); in contrast, deproteinized lariat RNA species can be quantitatively debranched (30). The observation that, in the nuclear extract, lariat RNAs contain a factor bound to the branch point (29) suggests that protection from enzymatic debranching is mediated by this RNA binding

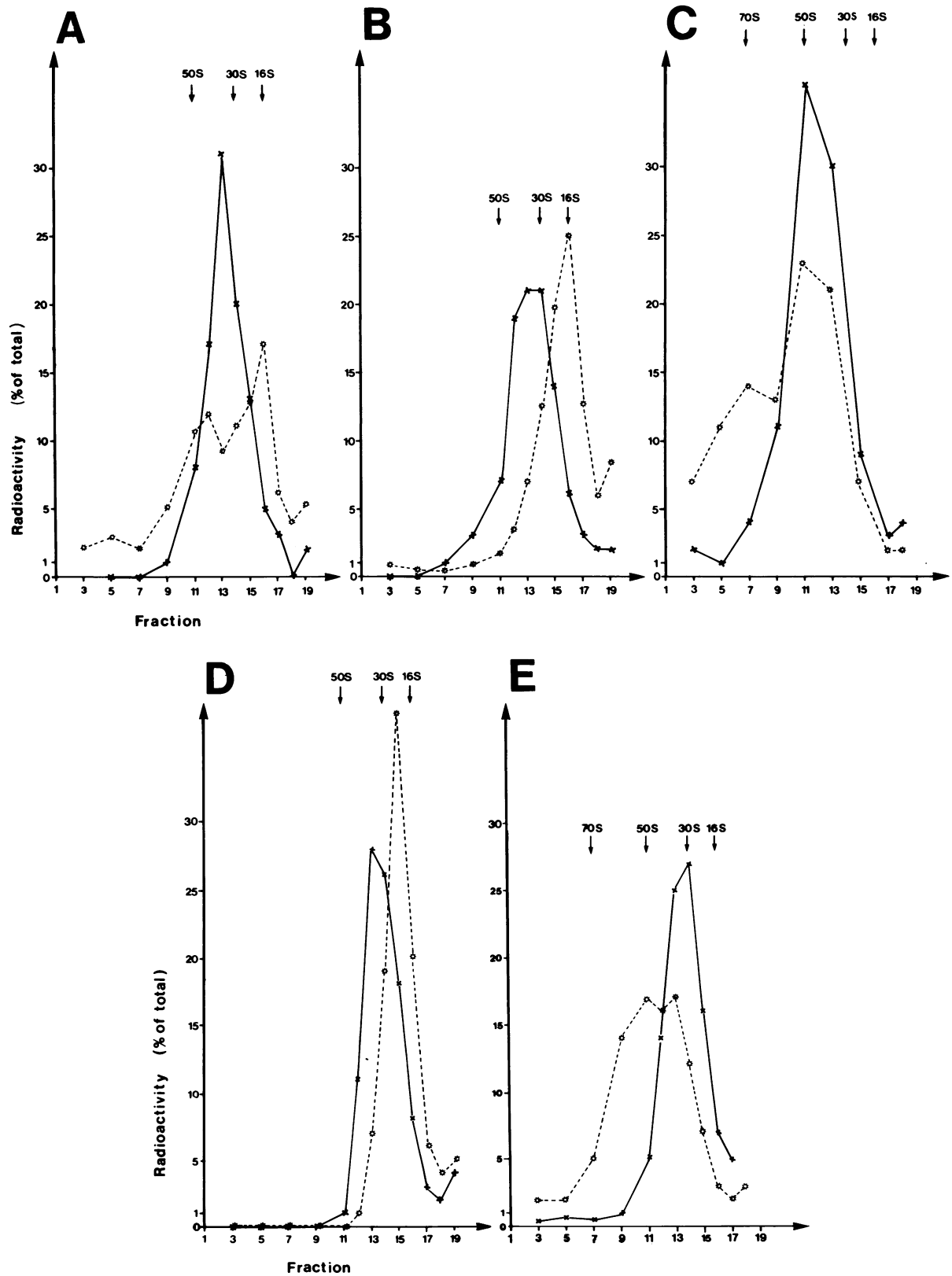

FIG. 2. ATP and sequence requirements of RNP complex formation. ^{32}P-labeled SP6-HβΔ6 (497 nts), SP6/Hβ$^{\Delta PyAG}$ (482 nts), and SP64 (519 nts) RNAs were synthesized in vitro and incubated for 45 min in HeLa cell nuclear extract under standard in vitro splicing conditions (16, 32), and the reaction mixture was analyzed by sucrose gradient centrifugation. The positions of the sedimentation markers are indicated above the panels. For the incubations shown in C, D, and E, PVA was omitted. RNA prepared from the gradient fractions was resolved by

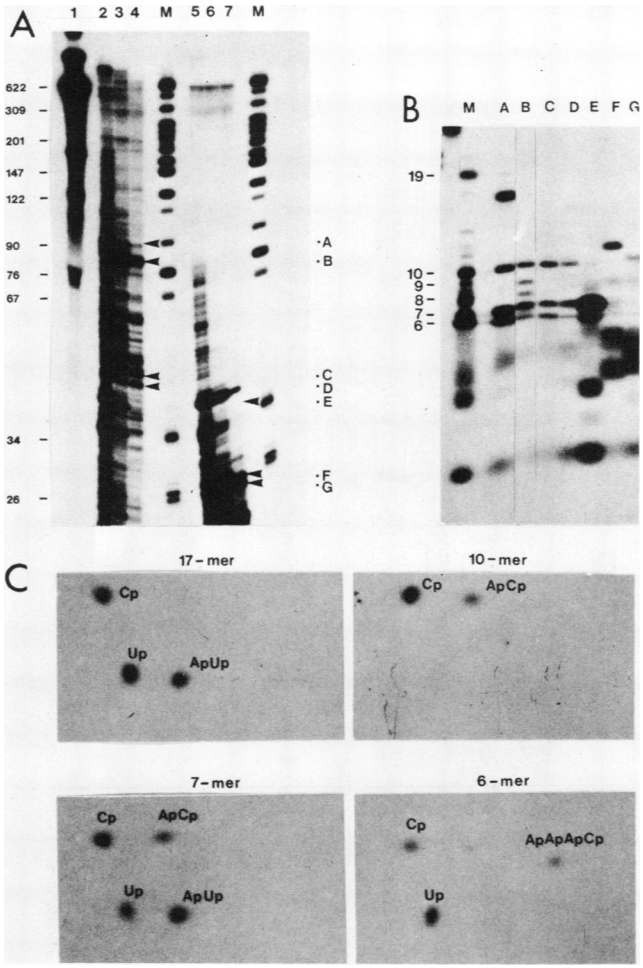

FIG. 3. Protection of pre-mRNA sequences in 60S RNP complexes from RNase A digestion. ^{32}P-labeled pre-mRNA complexes of approximately 60S (A, lane 1) were isolated from a 20-min in vitro splicing reaction mixture by sucrose gradient centrifugation. After partial RNase A digestion (10, 30, and 100 ng of RNase A in A, lanes 2 to 4 and 5 to 7, respectively) of RNP complexes (A, lanes 2 to 4) and RNA prepared from RNP complexes (A, lanes 5 to 7), protected RNA fragments (A, RNAs A to G) were purified by denaturing gel electrophoresis (12% acrylamide–8.3 M urea). The gel-purified, protected RNase A fragments were digested by RNase T1, electrophoresed on a 20% acrylamide–8.3 M urea gel, and detected by autoradiography (B, RNAs A to G). The gel-purified RNase T1 fragments were then further analyzed by secondary digestion with RNase A and two-dimensional thin-layer chromatography of the secondary digests on polyethyleneimine plates (first dimension, bottom to top; second dimension, right to left). (C) RNA A: 17-mer, UCUAUUUUCCCACCCUU, nts 254 to 270; 10-mer, ACUCUCUCUG, nts 236 to 245; 7-mer, ACUCUUG, nts 211 to 217, and CCUAUUG, nts 246 to 252; 6-mer, AAACUG, nts 185 to 190, and UUUCUG, nts 220 to 225 (17). ^{32}P-labeled, *Msp*I-digested pBR322 DNA (A, lane M) and the RNase T1 fragments of pre-mRNA (B, lane M) served as size markers.

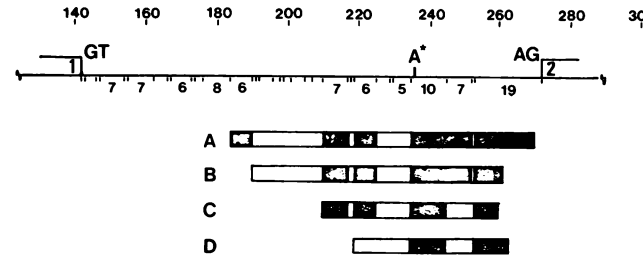

FIG. 4. Map of IVS1 RNA sequences protected in 60S pre-mRNA RNP complexes. A map of the RNase T1 cleavage sites within IVS1 (nts 143 to 272; 17) of the human β-globin pre-mRNA is given with the sizes of RNase T1 fragments 6 nts or longer and the branched adenosine residue (A*) indicated. The adjacent exon 1 and 2 sequences are represented by boxes. RNA sequences protected from RNase A digestion and derived from analyses of RNAs A to D (Fig. 3) are delineated. Sequences shown by shaded areas were identified by RNase T1 and RNase A analysis as described in Fig. 3.

factor(s). We used resistance to enzymatic debranching as an assay to determine whether the factor(s) that mediates branch point protection is retained in the isolated RNP complexes of the lariat RNA species.

Enzymatic debranching resulted in conversion of the deproteinized 380 and 143 RNA lariats to linear RNAs with electrophoretic mobilities of 339 and 130 nts, respectively (30; Fig. 5). To obtain partially purified RNP complexes containing lariat RNA species, we fractionated 90-min splicing reaction mixtures by sucrose gradient centrifugation at various salt concentrations and individually tested fractions at 60S, 50S, 30S, and smaller than 10S (Fig. 5). As controls, deproteinized RNA from the same gradient fraction and a mixture of gradient fraction and deproteinized RNA were assayed under identical conditions. Remarkably, the 380 RNA in the 60S RNP complex was completely resistant to enzymatic debranching, even when isolated from gradients that contain 0.9 M KCl. In contrast, resistant and sensitive forms of the 143 RNA RNP complex could be separated by sucrose gradient sedimentation. The 143 RNA RNP complexes sedimenting at 50S and 60S were predominantly resistant to enzymatic debranching, whereas 143 RNA RNP complexes sedimenting at or below 30S were debranched. Increasing the salt concentration to 0.5 or 0.9 M converted most or all, respectively, of the 143 RNA to a form that was sensitive to enzymatic debranching (15S RNP complex or free RNA).

RNP complexes contain snRNP-specific polypeptides. To begin to investigate the components of the RNP complexes, we determined whether they contained polypeptides from small nuclear RNP particles (snRNPs). A variety of studies have demonstrated that snRNPs are essential splicing factors whose mechanism of action involves binding to specific pre-mRNA regions (1, 4, 14, 15, 23, 26). Antibodies specific for either the Sm class of snRNPs (U1, U2, U4, U5, and U6 snRNPs; anti-Sm) or for U1 snRNP [anti-(U1)RNP] were used to probe for these components in the various RNP

denaturing gel electrophoresis and detected by autoradiography. Relative quantities of pre-mRNA in each fraction were determined and are represented as percentages of total pre-mRNA across the gradient. A, B, and D show the size distribution of RNP complexes of the normal pre-mRNA (pSP64-HβΔ6, A), the 3′ splice site deletion mutation pre-mRNA (pSP6/Hβ$^{\Delta PyAG}$, B), and SP64 RNA (D) in 60 (solid line) and 200 (broken line) mM KCl sucrose gradients. C compares the sedimentation profiles at 60 mM KCl of normal (broken line) and 3′ splice site mutant (solid line) pre-mRNA. E compares the sedimentation profiles at 60 mM KCl of normal pre-mRNA in the presence (broken line) and absence (solid line) of ATP-creatine phosphate.

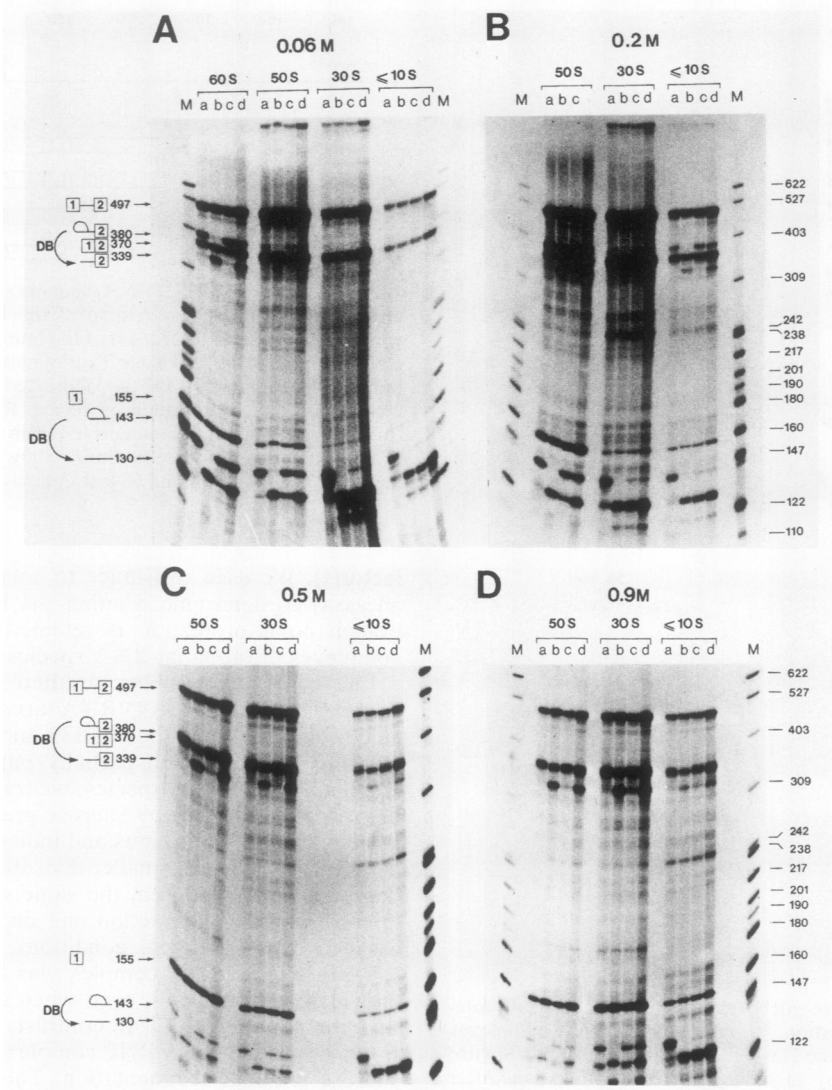

FIG. 5. Protection of lariat RNA species in RNP complexes from enzymatic debranching. Protection of the lariat RNA species (380 RNA, intron lariat-exon 2; 143 RNA, intron lariat) from enzymatic debranching was tested in gradient fractions collected from sucrose gradients in 0.06 (A), 0.2 (B), 0.5 (C), and 0.9 (D) M KCl. Gradient fractions from the 60S, 50S, 30S, and smaller-than-10S regions were chosen as representative samples. Pre-mRNA, splicing intermediates, and products, as well as the products of the enzymatic debranching (DB) reaction, are schematically represented (boxes 1 and 2, exons 1 and 2, respectively; line, intron). Purified RNA was resolved by denaturing gel electrophoresis using ^{32}P-labeled, *Msp*I-digested pBR322 DNA as markers (lanes M) and detected by autoradiography. For each gradient fraction, the RNA composition is shown (lanes a), as well as the RNA products after deproteinization and enzymatic debranching (lanes b) and after enzymatic debranching without prior deproteinization (lanes c). An additional control are the RNA products after enzymatic debranching of a 1:1 mixture of deproteinized gradient fraction and untreated gradient fraction (lanes d).

complexes. RNP complexes isolated by sucrose gradient sedimentation were immunoprecipitated with anti-Sm and anti-(U1)RNP specific antibodies, respectively, and the immunoprecipitated [^{32}P]RNA was purified and analyzed by denaturing gel electrophoresis (1; see Materials and Methods). The immunoprecipitation efficiency of the various RNP complexes was determined by comparing the total [^{32}P]RNA of gradient fractions to the [^{32}P]RNA obtained from the same fraction after immunoprecipitation with anti-Sm (Fig. 6) or anti-(U1)RNP (Fig. 7) antibodies. Several control human sera, lacking snRNP-specific antibodies, were tested and did not immunoprecipitate any of the [^{32}P]RNA species (data not shown).

Pre-mRNA RNP complexes purified from both the 60S and 40S regions of a 0.06 M sucrose gradient were efficiently immunoprecipitated by the anti-Sm antibody (Fig. 6). The RNP complex that contained the 380 and 155 RNAs was also efficiently immunoprecipitated (fractions 7 to 11). Equimolar recovery of the 380 and 155 RNAs in the immunoprecipitate argues that these two RNA species are held together in a single RNP complex. Similarily, RNP complexes containing the pre-mRNA and splicing intermediates isolated form 0.2 M KCl sucrose gradients were efficiently immunoprecipitated (Fig. 6B, fractions 11 to 15). Compared with the RNP complexes containing the pre-mRNA and splicing intermediates, the RNP complexes that contain accurately spliced RNA were immunoprecipitated inefficiently (Fig. 6A and B). This was particularly apparent when RNP complexes con-

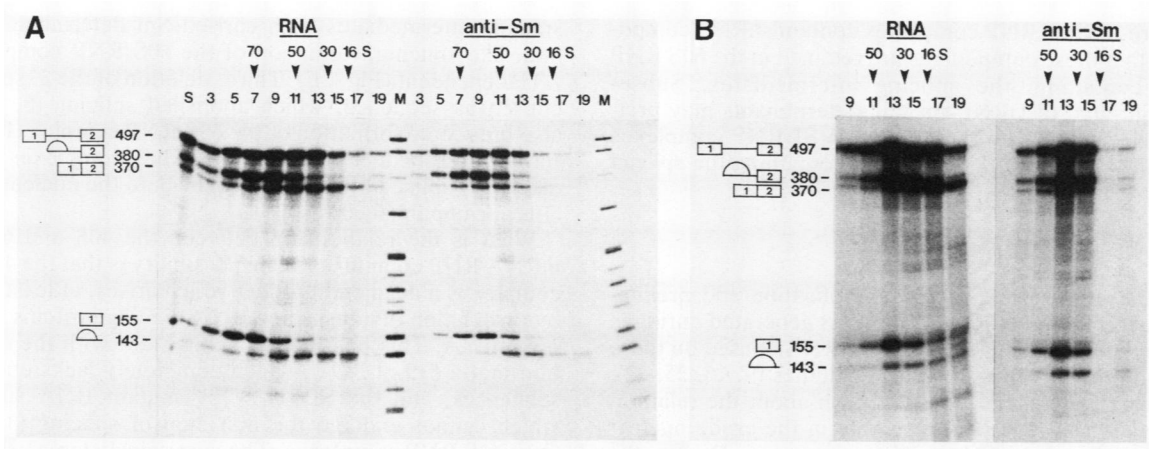

FIG. 6. Anti-Sm immunoprecipitation of purified RNP complexes. ^{32}P-labeled SP64-HβΔ6 RNA was spliced in vitro for 60 min and analyzed by sucrose gradient sedimentation at 0.06 (A) and 0.2 (B) M KCl. For RNA analyses (RNA in A and B), RNA prepared from a sample of the supernatant fraction of the total splicing reaction mixture before centrifugation (lane S) and from 20-μl aliquots of the gradient fractions (numbered 1 to 20 from the bottom to the top of the gradient) was resolved by denaturing gel electrophoresis using ^{32}P-labeled, *Msp*I-digested pBR322 DNA as markers (lanes M) and detected by autoradiography. The numbers of the gradient fractions and the positions of the sedimentation markers are indicated above the lanes. For anti-Sm immunoprecipitation analysis (anti-Sm in A and B), 100-μl samples of the gradient fractions were used for immunoprecipitations. RNA was prepared from the immunoprecipitates, resolved by denaturing gel electrophoresis, and detected by autoradiography. The diagrams on the left are explained in the legend to Fig. 1.

taining the spliced RNA, purified from 0.2 M KCl gradients, were analyzed by anti-Sm immunoprecipitation (Fig. 6B, lane 17).

RNP complexes containing the excised IVS1 displayed a characteristic pattern of anti-Sm immunoprecipitation. The larger forms (30S to 50S; Fig. 6A, fractions 11 to 13) were efficiently immunoprecipitated, whereas the smaller forms (<20S; Fig. 6A, fractions 15 to 17) were not. When the RNP complexes isolated from a 0.2 M KCl sucrose gradient were analyzed, the same result was obtained (Fig. 6B, compare fractions 13 to 15 with fractions 17 to 19). We noted that RNP complexes containing the excised IVS1 were more efficiently immunoprecipitated than the RNP complexes containing the spliced RNA product. For example, in fractions 11 to 13 the autoradiographic signal was higher for spliced RNA than for excised IVS1; in the immunoprecipitate the IVS1 signal was equal to or greater than that of the spliced RNA (Fig. 6A). A comparable pattern of immunoprecipitation was obtained with an independent anti-Sm antibody (data not shown).

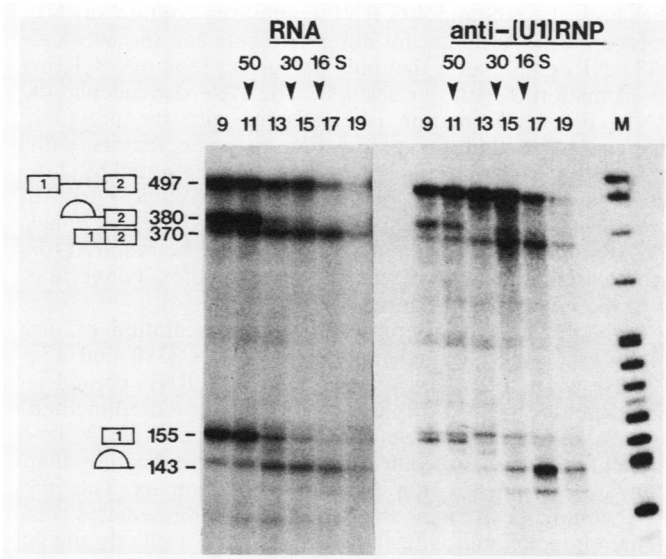

FIG. 7. Anti-(U1)RNP immunoprecipitation of purified RNP complexes. ^{32}P-labeled SP64-HβΔ6 RNA was spliced in vitro for 60 min and analyzed by sucrose gradient sedimentation. For RNA analysis (RNA), RNA prepared from 20-μl aliquots of the gradient fractions (numbered 1 to 20 from the bottom to the top of the gradient) was resolved by denaturing gel electrophoresis using ^{32}P-labeled, *Msp*I-digested pBR322 DNA as markers (lane M) and detected by autoradiography. The numbers of the gradient fractions and the positions of the sedimentation markers are indicated above the lanes. For anti-(U1)RNP immunoprecipitation analysis [anti-(U1)RNP], 100-μl samples of the gradient fractions were used for immunoprecipitations. RNA was prepared from the immunoprecipitates, resolved by denaturing gel electrophoresis, and detected by autoradiography. The diagram on the left is explained in the legend to Fig. 1.

To probe for the presence of (U1)RNP-specific polypeptides in the various RNP complexes, we repeated the immunoprecipitation analysis with an anti-(U1)RNP specific antibody (Fig. 7). RNP complexes containing the pre-mRNA were precipitated with the anti-(U1)RNP antibody; the 40S RNP complex was slightly more efficiently immunoprecipitated than the 60S RNP complex. Compared with the results with the anti-Sm antibody (Fig. 6), the RNP complexes containing the splicing intermediates were immunoprecipitated relatively inefficiently with the anti-(U1)RNP antibody (Fig. 7, fractions 9 to 11). RNP complexes containing the excised IVS1 also displayed a characteristic pattern of anti-(U1)RNP immunoprecipitation. A 15S RNP complex was most efficiently immunoprecipitated (fraction 17); RNP complexes containing the excised IVS1 that are larger (fractions 11 to 15) and smaller (fraction 19) than 15S were significantly less efficiently immunoprecipitated. We note that this 15S RNP complex was immunoprecipitated with the anti-Sm antibody relatively inefficiently (Fig. 6A and B, lanes 17). This same result was obtained in several independent experiments. A comparable pattern of immunoprecipitation was obtained with an independent anti-(U1)RNP antibody (data not shown).

Taken together, these results indicate that both the 40S

and 60S pre-mRNA RNP complexes contain snRNP components and that these components are retained in the 60S RNP complex containing the splicing intermediates. Subsequently, Sm- and (U1)RNP-specific determinants may preferentially segregate with the excised IVS1 RNP complexes rather than with the RNP complexes containing the spliced RNA.

DISCUSSION

In this paper we describe the identification and preliminary characterization of RNP complexes generated during in vitro splicing of an SP6/β-globin pre-mRNA. Based on these results and previous in vitro splicing studies (9, 16, 25, 32), the following conclusions can be drawn about the relationship between RNP complex assembly in the crude nuclear extract and the pre-mRNA splicing reaction. During the initial lag phase of the in vitro splicing reaction (11, 12, 16), the pre-mRNA is assembled into 40S and 60S RNP structures, the formation of which is ATP independent and dependent, respectively. As discussed below, it is likely that the 60S RNP complex is functional, giving rise to the two splicing intermediates that are also in a 60S RNP complex. The splicing intermediates go on to form the spliced RNA and the excised IVS1, which are in RNP complexes of 25S to 40S and 15S to 50S, respectively.

The differences between the reported sedimentation coefficients of the pre-mRNA RNP complexes in mammalian splicing systems (50S to 60S; 8, 10; our results) and the 40S pre-mRNA RNP complex detected in yeast cells (3) may be related to either differences in the biochemical components of the mammalian and yeast cell splicing complexes or experimental differences such as splicing or centrifugation conditions, length of pre-mRNAs, etc. With regard to mammalian splicing systems, we found that the RNP complexes of pre-mRNA, splicing intermediates, and products could be partially separated by sucrose gradient centrifugation. In contrast, most of the splicing-product RNP complexes derived from an adenovirus major late pre-mRNA appear to cosediment with the pre-mRNA and the splicing-intermediate RNP complexes at 50S and 60S, respectively (8, 10). The reason for this discrepancy is at present unclear but may be related to variations in experimental conditions. In one of the previous studies using an adenovirus major late pre-mRNA (8) it was reported that a 35S pre-mRNA RNP complex could be detected only during the initial 20 min of the splicing reaction. In contrast, we found that the presumably analogous 40S RNP complex was abundant at all times. This discrepancy may be due to variations in the extracts or the RNA substrates used in the two studies.

Analysis of RNP complex assembly of a deletion mutant (Fig. 2C) indicated that formation of a 60S pre-mRNA RNP complex is dependent on an intact 3′ splice site consensus sequence. A similar conclusion was reached using a deletion mutant derived from an adenovirus major late pre-mRNA (8). Additional evidence indicating that the 3′ splice site consensus sequence is required for splicing-complex formation is that deletion of this sequence prevents the specific association of a factor with the pre-mRNA branch point (29).

The following observations from this study strongly suggest that the 60S SP6/β-globin pre-mRNA RNP complex is the functional splicing substrate. First, the 60S pre-mRNA RNP complex cosedimented with the RNP complex that contained the two splicing intermediates (Fig. 1A). The 60S RNP complexes that contained the pre-mRNA and the splicing intermediates both carried Sm determinants. Second, like splicing, formation of the 60S RNP complex was ATP dependent (Fig. 2E). Third, deletion of the 3′ splice site consensus sequence, which abolished splicing (8, 27, 31), also prevented formation of the 60S RNP complex (Fig. 2C). Finally, purified 60S pre-mRNA RNP complexes can be efficiently spliced by adding them back to the nuclear extract (10; our unpublished results).

What is the relationship between the 40S and 60S pre-mRNA RNP complexes? One possibility is that the 40S RNP complex is a dead end product which arises, at least in part, by association of nonspecific RNA-binding proteins with the pre-mRNA. This possibility is consistent with the observation that a 519-nt RNA, which completely lacks eucaryotic sequences, and the SP6/H$\beta^{\Delta PyAG}$ mutant RNA substrate, which cannot undergo the first step of splicing (31), both form 40S RNP complexes. The surprisingly large size of the functional 60S RNP complex may result from both the association of nonspecific RNA-binding proteins with the pre-mRNA and the interaction of splicing factors that bind to specific pre-mRNA regions. It is at present not clear whether these putative sequence-nonspecific RNA-binding factors have any functional role in the pre-mRNA splicing reaction or are related to the well-characterized hnRNP core proteins (20). However, we note that, in contrast to the 40S hnRNP core particles (20), the RNP complexes containing the pre-mRNA and the splicing intermediates were not completely dissociated by 0.6 M KCl.

It is equally possible that the 40S RNP complex is an intermediate or an incompletely assembled pre-mRNA RNP complex. This possibility is consistent with the observation that both the 60S and 40S RNP complexes contain snRNP polypeptides. A significant difference between the 60S and 40S RNP complexes is that only the former requires ATP for its formation (8, 10; our results). The ATP dependence of RNP complex formation is consistent with the previous demonstration that the association of some factors with pre-mRNA has a specific ATP hydrolysis requirement (29). Perhaps ATP-dependent binding of splicing factors to the pre-mRNA converts the 40S RNP complex to the functional 60S RNP complex. Alternatively, ATP may be required for structural modification of the 40S RNP complex, converting it to the functional 60S form.

In contrast to the heterogeneous sedimentation of the pre-mRNA, the two splicing intermediates (380 and 155 RNAs) were found exclusively in a 60S RNP complex. Significantly, these two splicing intermediates cosedimented at salt concentrations of up to 0.9 M and were immunoprecipitated in equimolar quantities, indicating that they are contained within the same RNP complex. The 60S RNP complex containing the two splicing intermediates was immunoprecipitated with the anti-(U1)RNP antibody much less efficiently than with the anti-Sm antibody. This result could be due to either a lack of (U1)RNP determinants or, more likely, inaccessibility of U1(RNP) determinants to the antibody.

The RNP complexes containing the splicing products (370 and 143 RNAs) fractionated over a wide range, probably reflecting the gradual release of biochemical components, such as snRNPs, from these RNAs after splicing. The various 143 RNA RNP complexes displayed important structural differences. In contrast to the larger 143 RNA RNP complexes, the smaller 143 RNA RNP complexes were sensitive to enzymatic debranching and were not efficiently immunoprecipitated with anti-Sm antibody. Taken together, these results suggest that one or more Sm polypeptides may

be bound to the branch point of the RNA lariats, thereby protecting the 2'-5' phosphodiester bond from enzymatic debranching (30). The dissociation of factors from the branch point region of the 143 RNA RNP complex may be related to the in vivo intron degradation pathway. Excised introns (for an example, see reference 37), in particular 2'-5' phosphodiester bonds (36), do not accumulate in the nucleus in vivo. The factor that mediates branch point protection may dissociate from the excised intron (or be degraded in vivo) followed by cleavage of the 2'-5' phosphodiester bond by the lariat-debranching enzyme and then further nucleolytic degradation of the linearized introns. In fact linear forms of the excised intron have been detected in vivo in mammalian (37) and yeast (28) cells.

A final structural difference between the various 143 RNA RNP complexes was revealed by anti-(U1)RNP immunoprecipitation experiments. An intermediate-size 143 RNA RNP complex (15S) was most efficiently immunoprecipitated with the anti-(U1)RNP antibody. This result may reflect the unmasking of U1(RNP) determinants after dissociation of Sm determinants (or other factors) from the larger RNP complexes.

Based on RNA footprinting experiments, it has been previously shown that early during the pre-mRNA splicing reaction biochemical components associate with specific IVS1 regions and that these RNA-factor interactions are maintained in the IVS1-containing RNA processing products (29). The immunoprecipitation results presented here support and extend this conclusion. In the crude nuclear extract the pre-mRNA intron is associated with multiple snRNPs of the Sm class (1, 4). Consistent with this result, we and others (10) found that large RNP complexes containing the pre-mRNA were efficiently immunoprecipitated with the anti-Sm antibody. These Sm determinants are maintained in the RNP complex containing the 380 RNA splicing intermediate and appear to segregate preferentially with the excised IVS1 and not the spliced RNA product. Thus, the association of snRNP polypeptides that is established on the pre-mRNA is maintained in the IVS1-containing RNA processing products.

Our results indicate that sucrose gradient sedimentation is a useful method for isolating splicing complexes for further structural analysis. First, the various RNA species in both the crude nuclear extract (1, 10) and in sucrose gradient-isolated RNP complexes (10; our results) are associated with snRNP polypeptides. Second, the pre-mRNA branch point in both the crude nuclear extract (29) and the isolated RNP complexes (Fig. 3 and 4) is preferentially protected from RNase A digestion. Third, the 2'-5' phosphodiester bond of the lariat RNA species is protected from enzymatic debranching in both the crude nuclear extract (30, 32) and some of the sucrose gradient-isolated RNP complexes (Fig. 5). In this regard we noted that the 2'-5' phosphodiester bond in the RNP complex containing the 380 and 155 RNAs appeared to be more resistant to enzymatic debranching than in the 143 RNA complex. This result is not due to artifactual loss of biochemical components from the RNP complexes during gradient purification, since the two lariat RNA species displayed the same differential sensitivity to ionic strength in the crude nuclear extract (unpublished data).

A more detailed structural characterization of the individual RNP species should provide new insights into the pre-mRNA splicing mechanism. The RNA may be folded, by the interaction with snRNPs and other factors, into a splicing-competent RNP complex in which certain RNA regions are exposed, others are protected, and relevant regions to be recognized by the splicing machinery are brought into proximity.

ACKNOWLEDGMENTS

We thank V. Agnello for generously supplying human antisera. We thank Jim Grobholz for the preparation of nuclear extracts, members of the Green laboratory for critical comments on the manuscript, and Lee-Hsueh Hung for artwork.

A.B. was supported by a postdoctoral fellowship from the Deutsche Forschungsgemeinschaft. This work was supported by a Public Health Service grant from the National Institutes of Health to M.R.G.

LITERATURE CITED

1. **Black, D. L., B. Chabot, and J. A. Steitz.** 1985. U2 as well as U1 small nuclear ribonucleoproteins are involved in pre-messenger RNA splicing. Cell **42**:737–750.
2. **Breathnach, R., C. Benoist, K. O'Hare, F. Gannon, and P. Chambon.** 1978. Ovalbumin gene: evidence for a leader sequence in mRNA and DNA sequences at the exon-intron boundaries. Proc. Natl. Acad. Sci. USA **75**:4853–4857.
3. **Brody, E., and J. Abelson.** 1985. The 'spliceosome': yeast pre-messenger RNA associates with a 40S complex in a splicing-dependent reaction. Science **228**:963–967.
4. **Chabot, B., D. L. Black, D. M. LeMaster, and J. A. Steitz.** 1985. The 3' splice site of pre-messenger RNA is recognized by a small nuclear ribonucleoprotein. Science **230**:1344–1349.
5. **Contreras, R., H. Cheroutre, W. Degrave, and W. Fiers.** 1982. Simple, efficient in vitro synthesis of capped RNA useful for direct expression of cloned eukaryotic gene. Nucleic Acids Res. **10**:6353–6362.
6. **Domdey, H., B. Apostol, R. J. Lin, A. Newman, E. Brody, and J. Abelson.** 1984. Lariat structures are in vivo intermediates in yeast pre-mRNA splicing. Cell **39**:611–621.
7. **Efstratiadis, A., J. W. Posakony, T. Maniatis, R. M. Lawn, C. O'Connell, R. A. Spritz, J. K. DeRiel, B. G. Forget, S. M. Weissman, J. L. Slightom, A. E. Blechl, O. Smithies, F. E. Baralle, C. C. Shoulders, and N. J. Proudfoot.** 1980. The structure and evolution of the human β-globin gene family. Cell **21**:653–668.
8. **Frendewey, D., and W. Keller.** 1985. Stepwise assembly of a pre-mRNA splicing complex requires U-snRNPs and specific intron sequences. Cell **42**:355–367.
9. **Grabowski, P. J., R. A. Padgett, and P. A. Sharp.** 1984. Messenger RNA splicing in vitro: an excised intervening sequence and a potential intermediate. Cell **37**:415–427.
10. **Grabowski, P. J., S. R. Seiler, and P. A. Sharp.** 1985. A multicomponent complex is involved in the splicing of messenger RNA precursors. Cell **42**:345–353.
11. **Hardy, S. F., P. J. Grabowski, R. A. Padgett, and P. A. Sharp.** 1984. Cofactor requirements of splicing of purified messenger RNA precursors. Nature (London) **308**:375–377.
12. **Hernandez, N., and W. Keller.** 1983. Splicing of in vitro synthesized messenger RNA precursors in HeLa cell extracts. Cell **35**:89–99.
13. **Konarska, M. M., P. J. Grabowski, R. A. Padgett, and P. A. Sharp.** 1985. Characterization of the branch site in lariat RNAs produced by splicing of mRNA precursors. Nature (London) **313**:552–557.
14. **Kraemer, A., W. Keller, B. Appel, and R. Luehrmann.** 1984. The 5' terminus of the RNA moiety of U1 small nuclear ribonucleoprotein particles is required for the splicing of messenger RNA precursors. Cell **38**:299–307.
15. **Krainer, A. R., and T. Maniatis.** 1985. Multiple factors including the small nuclear ribonucleoproteins U1 and U2 are necessary for pre-mRNA splicing in vitro. Cell **42**:725–736.
16. **Krainer, A. R., T. Maniatis, B. Ruskin, and M. R. Green.** 1984. Normal and mutant human β-globin pre-mRNAs are faithfully and efficiently spliced in vitro. Cell **36**:993–1005.
17. **Lawn, R. M., A. Efstratiadis, C. O'Connell, and T. Maniatis.** 1980. The nucleotide sequence of the human β-globin gene. Cell

21:647–651.
18. **Lerner, M. R., J. A. Boyle, S. M. Mount, S. L. Wolin, and J. A. Steitz.** 1980. Are snRNPs involved in splicing? Nature (London) **283**:220–224.
19. **Lerner, M. R., and J. A. Steitz.** 1979. Antibodies to small nuclear RNAs complexed with proteins are produced by patients with systemic lupus erythematosus. Proc. Natl. Acad. Sci. USA **76**:5495–5499.
20. **Le Sturgeon, W. M., L. Lothstein, B. W. Walker, and A. L. Beyer.** 1981. *In* H. Busch (ed.), The cell nucleus, vol. 9. Academic Press, Inc., New York.
21. **Melton, D. A., P. A. Krieg, M. R. Rebagliati, T. Maniatis, K. Zinn, and M. R. Green.** 1984. Efficient in vitro synthesis of biologically active RNA and RNA hybridization probes from plasmids containing a bacteriophage SP6 promoter. 1984. Nucleic Acids Res. **12**:7035–7056.
22. **Mount, S. M.** 1982. A catalogue of splice junction sequences. Nucleic Acids Res. **10**:459–472.
23. **Mount, S. M., I. Petterson, M. Hinterberger, A. Karmas, and J. A. Steitz.** 1983. The U1 small nuclear RNA-protein complex selectively binds a 5′ splice site in vitro. Cell **33**:509–518.
24. **Padgett, R. A., S. F. Hardy, and P. A. Sharp.** 1983. Splicing of adenovirus RNA in a cell free transcription system. Proc. Natl. Acad. Sci. USA **80**:5230–5234.
25. **Padgett, R. A., M. Konarska, P. J. Grabowski, S. F. Hardy, and P. A. Sharp.** 1984. Lariat RNAs as intermediates and products in the splicing of messenger RNA precursors. Science **225**:898–903.
26. **Padgett, R. A., S. M. Mount, J. A. Steitz, and P. A. Sharp.** 1983b. Splicing of messenger RNA precursors is inhibited by antisera to small nuclear ribonucleoprotein. Cell **35**:101–107.
27. **Reed, R., and T. Maniatis.** 1985. Intron sequences involved in lariat formation during pre-mRNA splicing. Cell **41**:95–105.
28. **Rodriguez, J. R., C. W. Pikielny, and M. Rosbash.** 1984. In vivo characterization of yeast mRNA processing intermediates. Cell **39**:603–610.
29. **Ruskin, B., and M. R. Green.** 1985. Specific and stable intron-factor interactions are established early during *in vitro* pre-mRNA splicing. Cell **43**:131–142.
30. **Ruskin, B., and M. R. Green.** 1985. An RNA processing activity that debranches RNA lariats. Science **229**:135–140.
31. **Ruskin, B., and M. R. Green.** 1985. Role of the 3′ splice site consensus sequence in mammalian pre-mRNA splicing. Nature (London) **317**:732–734.
32. **Ruskin, B., A. R. Krainer, T. Maniatis, and M. R. Green.** 1984. Excision of an intact intron as a novel lariat structure during pre-mRNA splicing in vitro. Cell **38**:317–331.
33. **Seif, I., G. Khoury, and R. Dhar.** 1979. BKV splice sequences based on analysis of preferred donor and acceptor sites. Nucleic Acids Res. **6**:3387–3398.
34. **Treisman, R., S. H. Orkin, and T. Maniatis.** 1983. Structural and functional defects in β-thalassemia, p. 99–121. *In* G. Stamatoyannopoulos and A. H. Nienhuis (ed.), Globin gene expression and hematopoietic differentiation. Alan R. Liss, Inc., New York.
35. **Volckaert, G., and V. Fiers.** 1977. Microthin-layer techniques for rapid sequence analysis of ^{32}P-labeled RNA: double digestion and pancreatic ribonuclease analyses. Anal. Biochem. **83**:228–239.
36. **Wallace, J. C., and M. Edmonds.** 1983. Polyadenylated nuclear RNA contains branches. Proc. Natl. Acad. Sci. USA **80**: 950–954.
37. **Zeitlin, S., and A. Efstratiadis.** 1984. In vivo splicing products of the rabbit β-globin pre-mRNA. Cell **39**:589–602.